Selection of gp41-mediated HIV-1 cell entry inhibitors from biased combinatorial libraries of non-natural binding elements

Marc Ferrer[1], Tarun M. Kapoor[2], Tim Strassmaier[3], Winfried Weissenhorn[4,5], John J. Skehel[6], Dan Oprian[3], Stuart L. Schreiber[2,5], Don C. Wiley[1,4,5] and Stephen C. Harrison[1,4,5]

The trimeric, α-helical coiled-coil core of the HIV-1 gp41 ectodomain is thought to be part of a transient, receptor-triggered intermediate in the refolding of the envelope glycoprotein into a fusion-active conformation. In an effort to discover small organic inhibitors that block gp41 activation, we have generated a biased combinatorial chemical library of non-natural binding elements targeted to the gp41 core. From this library of 61,275 potential ligands, we have identified elements that, when covalently attached to a peptide derived from the gp41 outer-layer α-helix, contribute to the formation of a stable complex with the inner core and to inhibition of gp41-mediated cell fusion.

The attachment of enveloped viruses to cells and the fusion of viral and cellular membranes — the critical early events in viral infection — are mediated by envelope glycoproteins (gp) on the surface of the virus. The human immunodeficiency virus type 1 (HIV-1) envelope glycoprotein, gp160, is proteolytically cleaved into gp120 and gp41, which remain noncovalently associated with one another. Gp120 binds the cellular receptors and together with the membrane-spanning gp41 mediates the fusion of the viral and cellular membranes[1]. The gp120–gp41 complex undergoes conformational changes triggered by binding of gp120 with the cellular receptors[2–7], leading to activation of its membrane fusion properties[8–10].

The structure of a proteolytically resistant ectodomain of HIV-1 gp41 in the putative fusion-competent conformation has been determined[8–10]. Three gp41 subunits form a bundle of six helices. The core of the bundle is a parallel, triple-stranded, α-helical coiled-coil, made up of the gp41 N-terminus. Wrapped antiparallel on the outside of this core is an outer layer of three, C-terminal α-helices. This structure shares fea-

tures with fusion-mediating subunits of other enveloped virus glycoproteins, including the HA2 subunit of influenza virus[11], the F1 subunit of the paramyxovirus SV5[12–14], the GP2 subunit of Ebola virus[15,16], and the TM subunits of the retroviruses MuMoLV[17], HTLV-1[18,19], and SIV-1[20,21]. In all these cases, the fusion glycoprotein forms a rod-shaped α-helical bundle (reviewed by Skehel and Wiley[22]).

Triggered formation of the fusogenic conformation of the viral envelope protein appears to be a general mechanism of infection by several enveloped viruses[23]. Inhibition of this conformational activation is therefore an appealing general strategy for the treatment or prevention of viral infections[24–28]. In the case of HIV-1, peptides derived from predicted α-helical segments of gp41[27–29] have potent antiviral activity. In fact, one such peptide, DP-178, a 36-mer that includes part of the outer layer, C-terminal α-helix (residues Tyr 127–Phe 162), has been shown in clinical trials to reduce HIV-1 to undetectable levels[30]. The structure of the gp41 ectodomain has confirmed that these peptides correspond to parts of the outer layer, C-termi-
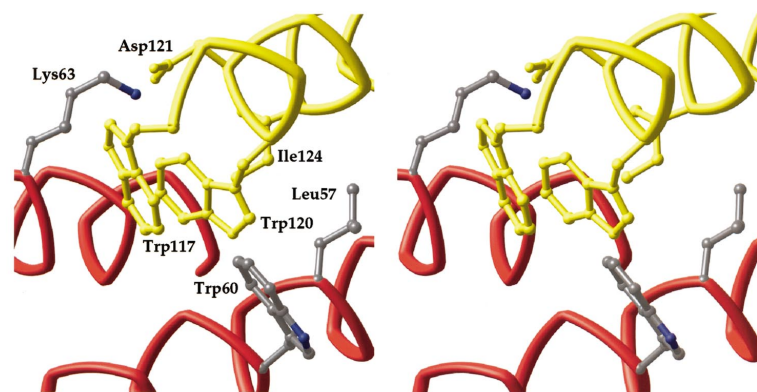

Fig. 1 Stereo view of contacts near the N-terminus of the outer helix of gp41. Two turns at the N-terminal end of the outer helix project Trp 117, Trp 120, and Ile 124 into a cavity on the surface of the coiled coil inner core including residues Leu 57 and Trp 60. A salt bridge between Asp 121 of the outer helix and Lys 63 on the inner core surface is also shown. Figure made with the program RIBBONS[47], using coordinates from Weissenhorn and colleagues[9].

[1]Department of Molecular and Cellular Biology, Harvard University, 7 Divinity Ave., Cambridge, Massachusetts 02138, USA. [2]Department of Chemistry and Chemical Biology, Harvard University, 16 Oxford St., Cambridge, Massachusetts 02138, USA. [3]Department of Biochemistry, Brandeis University, 415 South St., Waltham, Massachusetts 02454, USA. [4]Laboratory of Molecular Medicine, The Children's Hospital, 320 Longwood Ave., Boston, Massachusetts 02215, USA. [5]Howard Hughes Medical Institute. [6]National Institute for Medical Research, The Ridgeway, Mill Hill, London, NW7 1AA, UK.

Correspondence should be addressed to S.C.H. *email: schadmin@crystal.harvard.edu*
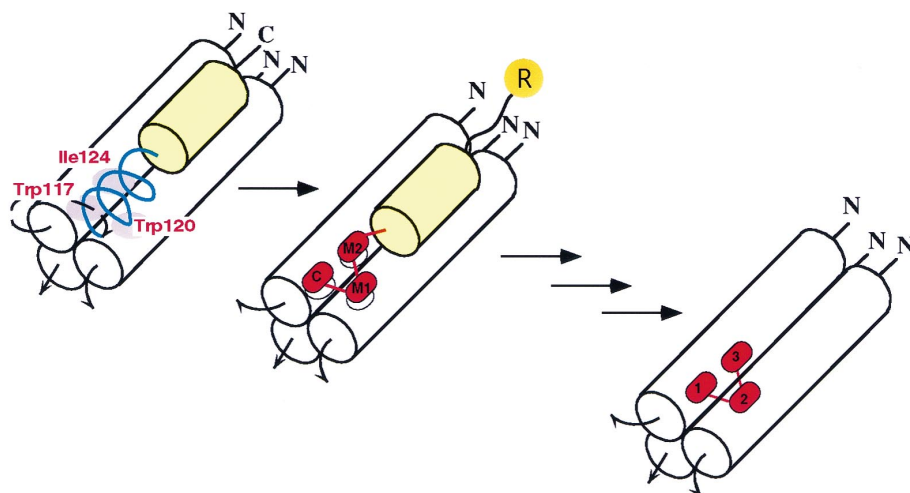
articles

Fig. 2 A structure-based combinatorial approach to identifiy inhibitiors of gp41-mediated viral entry. A fragment of the gp41 outer helix peptide is attached to the bead (R) and used to target a three-position non-peptide library into a hydrophobic cavity (purple ovals) on the surface of the inner coiled coil (middle). C, M1 and M2 (red ovals) represent the three library positions — cap, monomer 1 and monomer 2, respectively. The cavity is occupied in the original gp41 structure by residues Trp 117, Trp 120, and Ile 124 (left). Ultimately, the non-natural elements in the three library positions will be optimized to produce an inhibitor without the native peptide sequence (right).

nal α-helix. The structure suggests that these peptides block fusion by binding to the surface of the trimeric, coiled-coil inner core of gp41 and preventing the formation of the fusion-active six-helix bundle structure. Thus, the surface of the trimeric, coiled-coil inner core of gp41 appears to be a valid target for the design of ligands with anti-viral activity. Furthermore, the amino acid side chains on the surface of the inner core are highly conserved, a likely consequence of their role in assembly of a fusion-competent structure. This observation suggests that the amino acids on the surface of the core may be more constrained in their ability to undergo drug-resistance mutations.

The structure of the gp41 ectodomain shows that there is a deep cavity on the surface of the inner core, which might be targeted by small molecule inhibitors[8] (Fig. 1). This cavity lies near sites implicated by mutagenesis in fusion activity[31–33]. It is formed by residues surrounding amino acids Leu 57, Trp 60, and Lys 63 on the inner layer helix, and it is occupied in the gp41 structure by residues Trp 117, Trp 120, and Ile 124 on the outer layer α-helices. The effects of mutations in the last three residues confirm that they contribute to the stability of the core and to fusion activity[33], although the role of other residues along the outer helix that also contribute to the buried interface was not tested.

We have initiated efforts towards the discovery of small organic inhibitors that block gp41 activation by generating and screening biased combinatorial chemical libraries targeted

to the trimeric core. The use of structural information of a receptor–ligand complex to guide the design of combinatorial libraries of non-natural binding elements has been successfully applied to identify SH3 domain ligands[34,35]. We have combined the insights gained from the gp41 X-ray structures, analysis of the effects of mutations on fusogenic activity, and biophysical and biochemical analyses of the peptide inhibitors, to design a combinatorial library of non-natural binding elements targeted to interact with the cavity on the surface of the inner core described above. The strategy we have followed is shown in Fig. 2. A peptide with a sequence corresponding to residues Asn 125–Gln 142 of the gp41 outer helix was used as the biasing element. The combinatorial library of non-natural binding elements was synthesized on the N-terminus of this peptide, replacing amino acids Trp 117–Ile 124.

Design, synthesis and screening of a biased library

Using split-pool synthesis[36] compatible with recursive deconvolution[37], we generated a library of 61,275 potential ligands attached to the N-terminus of the biasing peptide. We developed a colorimetric, affinity-based selection assay and used it to evaluate the interaction of the gp41 inner core with thousands of immobilized compounds simultaneously. A protein with the sequence corresponding to the α-helical inner core of the gp41 ectodomain was the target for screening the library. The 'naked' gp41 inner core has a strong tendency to aggregate, however[38]. We therefore used a chimeric protein consist-
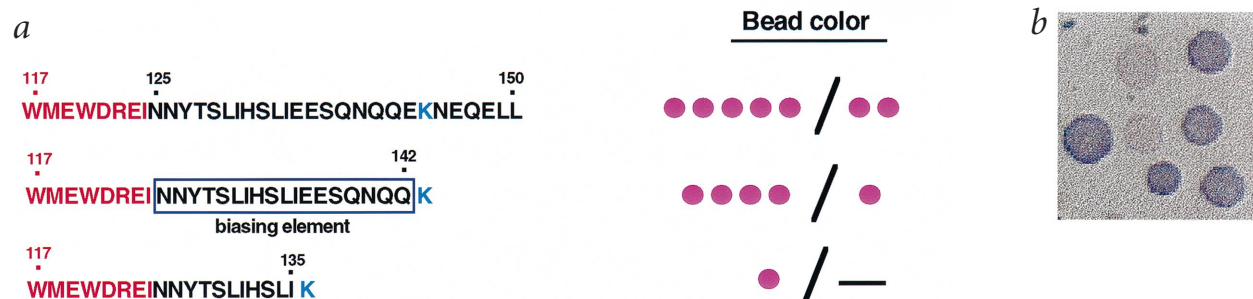

Fig. 3 Optimization of an on-bead affinity-based assay for the determination of a biasing peptide sequence. *a*, Color deposition on the bead was measured (scores were assigned visually) for a series of peptide pairs with and without the sequence between Trp 117 and Ile 124 (WMEWDREI, in red). Peptides were chemically synthesized, purified, and reattached to the solid support though the amine side chain of a Lys residue (K in blue). *b*, Photograph showing the difference in color between beads carrying the biasing element (lighter color), and beads carrying the biasing peptide with the Trp-rich sequence (darker color).
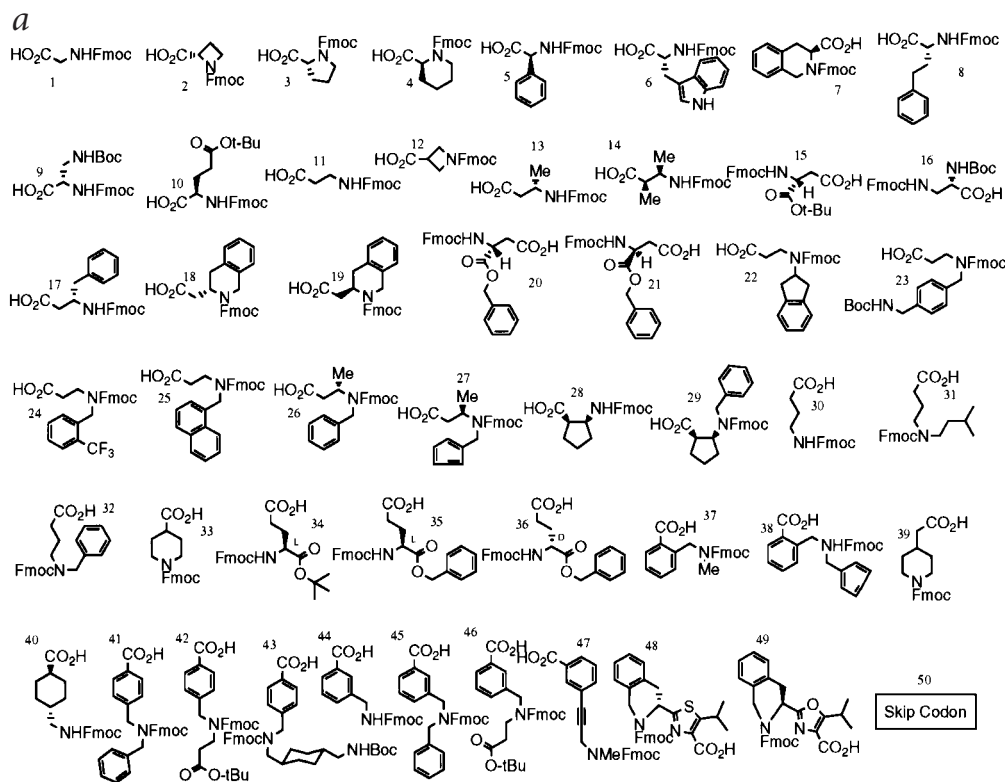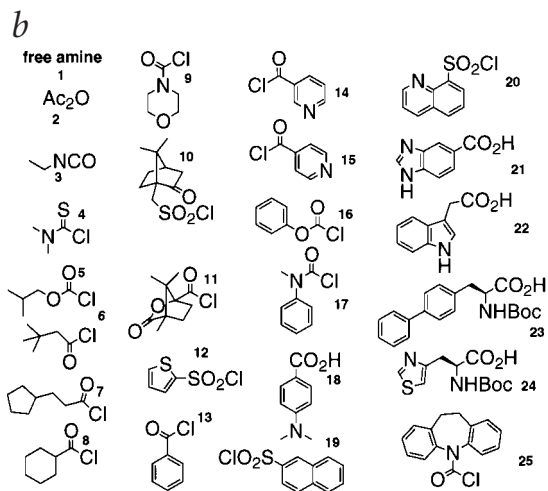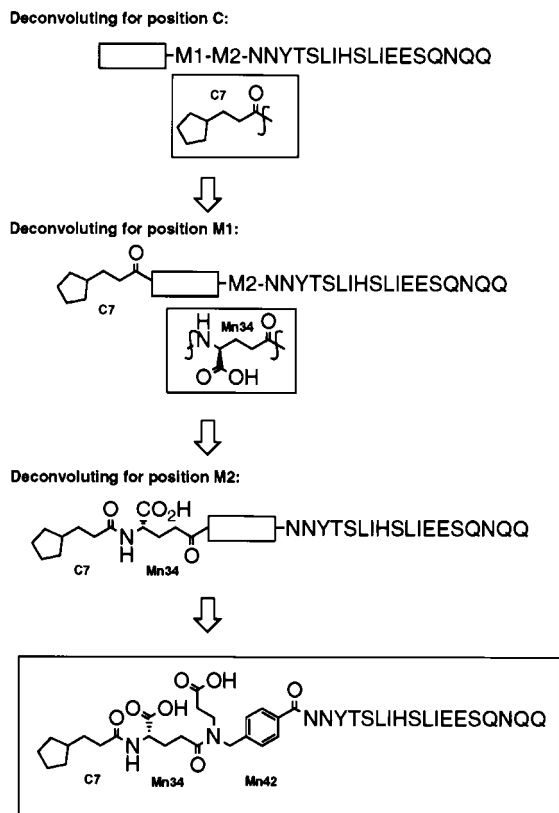
a

b

Fig. 4 Building blocks used to construct the library. *a*, Monomers (Mni) used at positions at M1 and M2. *b*, Capping agents (Ci) used at position C.

ing of a GCN4-like trimeric coil in register with the gp41 inner core α-helix. This chimeric molecule folds correctly with the gp41 outer helix, as shown by crystallographic studies[9], and it has allowed us to obtain a soluble, monodispersed species, as determined by HPLC size exclusion and sedimentation equilibrium analysis (data not shown). The protein target was biotinylated through a cysteine that was engineered at the N-terminus of the GCN4 moiety, on the opposite end of the molecule from the targeted site. To detect ligand binding, the biotinylated gp41 inner core was incubated with streptavidin-alkaline phosphatase conjugate (SA-AP) and added to the library of ligand-carrying beads. Subsequent incubation with alkaline phosphatase substrate produced insoluble blue dye on those ligand-carrying beads that had taken up the gp41 inner core.

To determine whether color intensity correlated with the length of the peptide and hence with the strength of binding the following controls were carried out. Color deposition on the bead was measured for a series of peptide pairs with and without the sequence between Trp 117–Ile 124 (WMEWDREI). These residues will be substituted by non-natural binding elements in the library. Three pairs of peptides (Fig. 3*a*) were synthesized, purified, and recoupled to beads by amide formation between a Lys side chain from the peptide and an activated carboxylate group on the resin. Under the conditions of the assay, beads containing a peptide with residues Trp 117–Leu 150, corresponding to almost the full length of the outer-layer α-helix, showed a very intense color (and hence a high efficiency of inner-coil binding). The similar peptide lacking the first eight N-terminal residues gave a lighter color. Another pair of shorter peptides, truncated at Gln 142, gave intense color for the long sequence, amino acids Trp 117–Gln 142, and very weak color for the peptide lacking the eight N-terminal residues. In the shortest pair of peptides tested, the long peptide, Trp 117–Ile 135, gave a very weak signal and the peptide lacking the eight N-terminal residues gave no detectable signal. The specificity of the interaction between the outer-layer α-helical peptides tethered to the beads and the gp41 region on the target chimeric protein was confirmed by competition with soluble, full length outer-helix peptide (Trp 117–Leu 150). Addition of the soluble peptide abolished color formation on beads carrying the peptide Trp 117–Leu 150 (data not shown) demonstrating that the bead-tethered peptide was not interacting with the GCN4 moiety of the target protein. Together, these results show that color deposition on the beads increases with the length of the peptide and with the presence of the Trp-rich sequence. If we assume that color intensity is a measure of affinity, these findings confirm the importance of the Trp-rich region at the N-terminus of the gp41 outer helix for binding to the inner core.

articles

Fig. 5 Results of deconvoluting the library of non-peptide elements biased to interact with the gp41 inner core. The empty box represents the unknown monomer at the position being deconvoluted. The deconvolution proceeded as follows. At the end of the library synthesis, we generated 25 discrete pools (one for each cap) of ~2,500 (50 M1 × 50 M2) compounds each. The pools of beads were screened visually for binding to the gp41 inner core/SA-AP reporter, and in parallel, to the SA-AP reagent alone, in order to test for potential false positives. Four C reagent pools (of the 25 capped pools) contained the darkest beads with the fewest false positives (SA-AP binders). Rescreening under more stringent conditions revealed the cyclopentyl propionyl group (C7 in Fig. 4b) as the one that contributes most to the gp41 interaction. To deconvolute position M1, 50 discrete portions of beads with ligands from an uncapped sub library containing M1-M2-bias-resin (reserved prior to coupling the capping reagent during library synthesis), were all capped with the cyclopentyl propionyl group (C7). Assays with biotinylated gp41 inner core/SA-AP and SA-AP alone selected glutamic acid coupled through its side chain (Mn34 in Fig. 4a) as the optimal building block at position M1. Finally, 50 discrete portions from a sub-library containing M2-bias-resin (reserved prior to coupling the position M1 monomers during library synthesis) were all reacted with Mn34 and C7 to yield 50 pools of C7-Mn34-M2-bias-resin. Assays with biotinylated gp41 inner core/SA-AP and SA-AP alone selected 4-(3-carboxyethyl) aminomethylbenzoic acid (Mn42 in Fig. 4a) as the optimal monomer at position M2. The binding specificity of the selected non-natural molecule (C7-Mn34-Mn42-biasing peptide-resin) for the gp41 inner core sequence on the target protein was confirmed by competing with soluble peptide Trp 117–Leu 150 (data not shown).

We also tested these peptides for inhibition of gp41-mediated cell fusion activity in a cell-cell fusion assay (Table 1). Inhibitory activity increased with the length of the peptide and the presence of the Trp-rich sequence, validating our screening strategy, which assumes that the affinity will correlate with inhibition.

From the on-bead affinity assay and the cell-cell fusion results, we selected the peptide Asn 125–Gln 142 (NNYTSLIH-SLIEESQNQQ) as a biasing element. This was the shortest peptide starting at Asn 125 for which incorporating the Trp-rich sequence resulted in a large difference in both on-bead affinity (Fig. 3a,b) and cell-cell fusion inhibition (Table 1). A three position (C-M1-M2) library of 61,275 unique compounds was generated by a split-pool synthesis compatible with recursive deconvolution. The building blocks for positions M1 and M2 (monomers, Mni, Fig. 4a) included non-natural amino acids that could be linked by amide bonds. They were selected to take advantage of hydrophobic contacts in the targeted pocket and to ensure that the relative orientation of hydrophobic groups in two monomers in a ligand was as variable as possible (Fig. 4a). A total of 8% of the monomers were negatively charged; these were introduced to take advantage of potential electrostatic interactions, particularly those seen in the structures between Lys 63 on the inner core and Asp 121 on the outer-layer α-helix. Two positively charged monomers were also included to increase diversity. The capping reagents (Ci) used in position C included compounds likely to mimic the indole group of Trp 117 (Fig. 4b). The results of the deconvolution procedure with the colorimetric affinity-based assay described above are summarized in Fig. 5.

Hybrid ligand and gp41 inner core form stable complex
The trimeric inner core is a soluble oligomeric, monodispersed species over a very limited range of concentrations, and

we have therefore been unable to develop a binding assay for determining the affinity of soluble outer-helix peptides. Instead, we have used *in vitro* refolding of inner-layer and outer-helix gp41 peptides[38] as a measure of their association in solution. The hybrid ligand identified from the library (C7-Mn34-Mn42-Asn 125–Gln 142), which contains an 18-residue segment portion of the 38-residue outer-layer α-helix, does not (off the beads) refold into a stable complex with the gp41 inner core *in vitro*. However, when the peptidic portion of the hybrid ligand was lengthened to 30 residues (Asn 125–Lys 154), a stable complex did form. The refolded hybrid gp41-like molecule eluted as a single species on gel filtration chromatography (Fig. 6a), migrated as a single band on nondenaturing polyacrylamide gel electrophoresis (PAGE) (Fig. 6b), and crystallized. The 30-residue peptide, Asn 125–Lys 154, alone did not form a stable complex with the gp41 inner-layer peptide. We conclude that the non-peptide elements interact with the inner-layer surface, increasing the binding affinity of the 30-mer peptide for the gp41 inner-layer. The observation that the 38-residue peptide forms stable gp41 structures, while the 30-mer without the non-natural binding element does not, demonstrates the importance of the Trp-rich region (Trp 117–Ile 124) at the N-terminus of the outer-layer α-helix for stable interaction with the inner core.

Inhibition of gp41-mediated cell fusion by hybrid ligands
We used a cell-cell fusion assay to measure the capacity of the identified ligands to inhibit gp41-mediated cell membrane fusion. (Table 1; Fig. 7). DP-178 (Tyr 127–Phe 162), the peptide corresponding to a segment of the outer-layer α-helix originally described to have anti-viral activity[28,39], was used as a positive control. In our cell fusion assay, DP-178 has an EC$_{50}$ of 50 nM.

The full length outer layer α-helix peptide, p38 (Trp 117–Lys 154), the hybrid ligand with the N-terminal eight residues replaced by C7-Mn34-Mn42 (C7-Mn34-Mn42-Asn 125–Lys 154) and the peptide with the N-terminal eight residues absent, p30 (Asn 125–Lys 154), had EC$_{50}$ values of 3 nM, 0.3 μM, and 7 μM, respectively (Table 1). Thus removing the N-
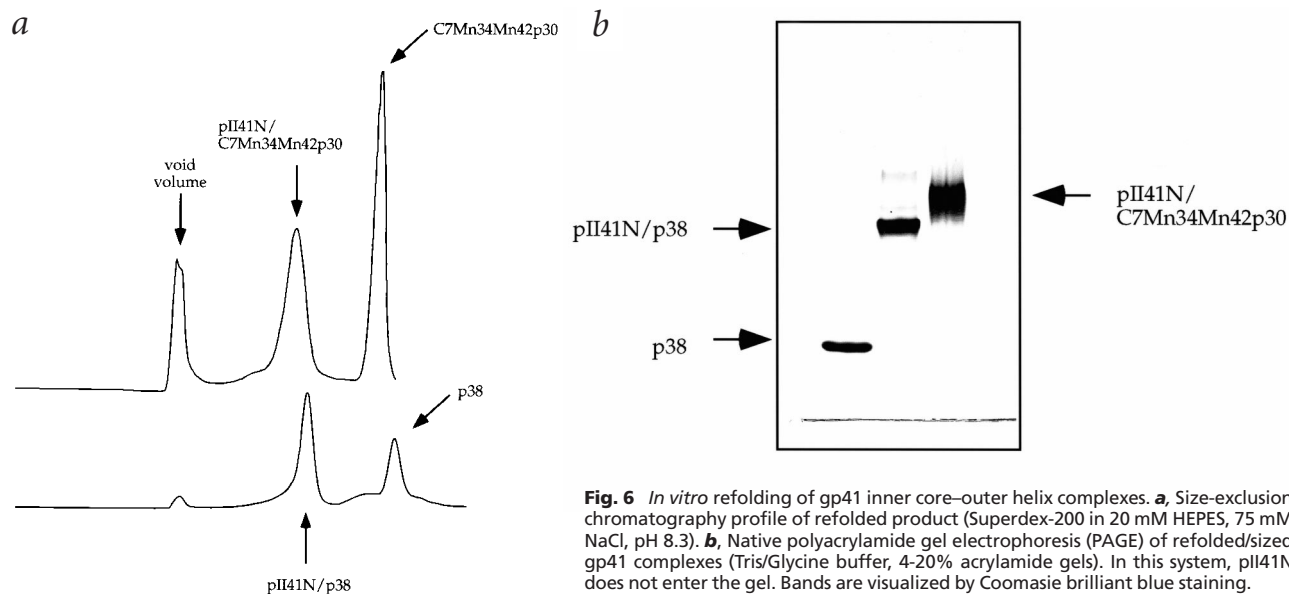
a

b

Fig. 6 *In vitro* refolding of gp41 inner core–outer helix complexes. **a**, Size-exclusion chromatography profile of refolded product (Superdex-200 in 20 mM HEPES, 75 mM NaCl, pH 8.3). **b**, Native polyacrylamide gel electrophoresis (PAGE) of refolded/sized gp41 complexes (Tris/Glycine buffer, 4-20% acrylamide gels). In this system, pII41N does not enter the gel. Bands are visualized by Coomasie brilliant blue staining.

terminal eight residues reduces the inhibition ~2,500-fold (3 nM to 7 µM for p30), and replacing the eight residues with the non-natural moiety C7-Mn34-Mn42 restores inhibition by only ~20-fold (7 µM to 0.3 µM). These data indicate that although the combinatorial moiety interacts sufficiently strongly when coupled to a peptide to form a stable complex with the inner core, it interacts about a 100-fold more weakly than the native amino acid sequence. This may indicate that the non-natural portion makes fewer contacts than anticipated — a proposal that can be directly tested by determining the structure of the crystallized complex.

The peptide p26 (Table 1), Trp 117–Gln 142, that corresponds to the biasing element plus the Trp-rich region, has an EC_{50} of 3 µM. The biasing peptide alone, amino acids Asn 125–Gln 142 (p18) showed no detectable inhibition at concentrations up to 200 µM. C7-Mn34-Mn42-p18, the hybrid ligand isolated from screening the library, also did not have inhibitory activity at concentrations up to 200 µM. These results confirm that the eight N-terminal residues are critical for the inhibitory activity of a peptide as short as p26. Furthermore, the observation that p26, containing the N-terminal eight residue, Trp-rich region, is a slightly more potent inhibitor than p30 (3 µM to 7 µM) which lacks the Trp-rich region but contains 12 residues at the C-terminus, suggests that both terminal sequences of the outer layer helix fragment Asn 125–Gln 142, provide similar binding energy to the inner core.

Mechanism of inhibition by outer-layer peptides
The trimeric core of gp41 is likely to be part of a transient intermediate in the folding of gp41 to a fusion-active conformation. Inhibitors such as DP-178 are thought to bind to this transient intermediate, causing misfolding of gp41 during the transition to a fusion active state[8,9,38,40,41]. Here, we show that it is possible to obtain ligands to the intermediate transient state, and that these ligands can improve inhibitory activity.

We have observed that the peptide p38, and the hybrid ligand, C7-M34-M42-p30, are more potent inhibitors of cell-cell fusion than the peptide p30, which lacks the Trp-rich sequence from Trp 117–Ile 124. These results suggest that the target

sequence of the inner core — residues near Leu 57, Trp 60, and Lys 63 (Fig. 1), which are covered by the Trp-rich sequence in gp41 — is exposed and available at some stage during the gp41-mediated membrane fusion. The effects of mutations in the last three residues show that this segment also contributes to the stability of the gp41 core[33]. The roles of other residues along the outer helix that contribute to the buried interface have not been tested.

The relative inhibitory capacities of DP-178 (Tyr 127–Phe 162; 60 nM) and p38 (Trp 117–Lys 154, 3 nM) suggest that the ten N-terminal residues unique to p38 interact more strongly with the core than do the eight C-terminal residues unique to DP-178. This result is consistent with proteolysis experiments[38,42,43] and with the gp41 structures[8–10]. The N-terminal residues contained in p38 have stable helical contacts, while the C-terminal residues contained in DP-178 are proteolytically sensitive, presumably due to contacts beyond Lys 154. By selecting resistant virus that grows in the presence of the inhibitory peptide DP-178, part of its target site has been localized to residues Gly 36 and Val 38 near the N-terminus of the inner-core α-helices[44]. The three-dimensional structure of gp41 shows that Gly 36 and Val 38 contact residue Asn 145 on the outer helix, which is present in DP-178, but it remains unclear by what mechanism the Trp-rich sequence at the C terminus of DP-178 confers anti-viral activity and fusion-inhibitory activity on an otherwise inactive peptide (p30). It might enhance binding of p30 to the inner core, as does the N-terminal sequence present in p38. Structural information about the mechanism of such an enhancement is not available, however, since the gp41 inner core residues that would be opposite this segment are missing from the various fragments studied crystallographically.

Conclusions and prospects
We have designed and generated a biased combinatorial library of non-natural elements targeted to the surface of the gp41 inner core, to identify small molecules that prevent viral entry by blocking gp41 activation. Affinity selection has identified non-natural elements that contribute, when covalently attached to a peptide derived from the outer-layer α-helix, to
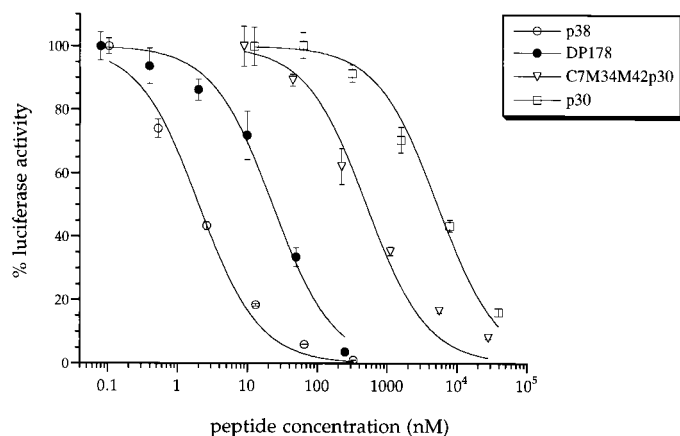
articles

Fig. 7 Inhibition of gp41-mediated cell-cell fusion by outer helix peptides and peptide-hybrids. Inhibition of fusion between cells expressing HIV-1 gp160 and cells expressing CD4 by DP-178 (closed circles), p38 (open circles), p30 (open squares), and C7-Mn34-Mn42-p30 (open triangles). Vertical bars indicate standard deviations of the mean of triplicate samples.

formation of a stable complex with the inner core and to inhibition of gp41-mediated cell fusion.

The observation that the shorter hybrid ligand, C7-Mn34-Mn42-p18 (p18 being the biasing element used to construct the library) binds to the trimeric gp41 inner core when attached to a bead, but not when free in solution, suggests that multiple interactions are needed to capture the probe. That is, our affinity selection procedure was probably in practice an avidity assay, leading to detection of rather weakly binding ligands. To improve the bead assay, we are now constructing a gp41 target in which tow of the three grooves of the surface of the trimeric inner core are occupied by covalently attached C-terminal helices, and only one is free to interact with a potential ligand from a biased library. This gp41 variant should provide a monovalent probe for library screening. We also expect that the two outer layer helices will stabilize the variant and it will therefore not dissociate at low concentrations (nM). By lowering the concentration of target protein we expect to increase further the stringency of the screen.

Methods
Peptide synthesis. Peptides were synthesized with an Applied Biosystems Peptide Synthesizer (Model 431A) using standard solid-phase Fmoc chemistry on a PAL-support (Perseptive Biosystems, MA), that yields peptide amides. Peptides were cleaved using TFA/5% phenol/5% H_2O/5% thioanisole/2.5% 1,2-ethanedithiol (10 ml, for 2 h) and purified with HPLC on a C-18 reversed phase column (Vydac, CA) using a triethylamine acetate, pH 5.9/acetonitrile buffer system. Peptides were characterized by electrospray mass spectrometry at the Mass Spectrometry Facility

in the Department of Chemistry and Chemical Biology at Harvard University.

Preparation of biotinylated gp41 inner core. The pII41N-Cys construct[41] was used to obtain the trimeric gp41 inner core for screening the library of non-natural ligands. This protein construct contains 31 residues of pIIGCN4, and residues Ala 30–Gln 79 from the HIV-1 gp41 inner coil. Residue Ser 13 of pIIGCN4 was mutated to cysteine. pII41N-Cys was expressed in *E.coli* BL21 DE3/pUBS. Inclusion bodies were washed as described in Weissenhorn *et al.*[41] and solubilized in 6 M GdmHCl, and 20 mM DTT buffer. Refolding was carried out by diluting 1/50 in 20 mM HEPES, 50 mM NaCl, 1 mM DTT, 0.6 M GdmHCl, pH 6.5, and dialyzing against 20 mM HEPES, 50 mM NaCl, pH 7.0 at 4 °C (2 × 8 h). Biotinylation of the cysteines was carried out with biotin-maleimide (Molecular Probes), which was dissolved in DMSO and added to the protein solution at ~10-fold molar excess over monomeric protein. Coupling was carried out overnight at 25 °C. The protein solution was then dialyzed against PBS (3 × 8 h) at 4 °C, and concentrated to ~15 μM. Biotinylation was confirmed by Western blotting with streptavidin-alkaline phosphatase.

Peptide resins for optimization of the on-bead affinity-based selection assay. Peptides were attached to the solid support by amide bond formation between an activated carboxylic acid on the solid support and an amine from a Lys on the peptide. The Lys residues were at the C-terminus or placed in the sequence at an exposed position (Fig. 3*a*). In a typical synthesis, 200 mg of TentaGel S NH_2 (RAPP Polymere, 0.25 mg ml⁻¹, 80 mm) were treated with succinic anhydride (4 equiv, 0.2 mmol), and DIEA (8 equiv, 0.4 mmol) in 1 ml DMF for 2 h. The resin was drained, washed with CH_2Cl_2 (5 ml × 3), DMF (5 ml × 3), CH_2Cl_2 (5 ml × 3), and dried overnight in a vacuum desiccator. 5 mg (~0.00125 mmol) of this resin was then treated with N-hydroxy succinimide (10 equiv, 0.0125 mmol) and diisopropylcarbodiimide (10 equiv, 0.0125 mmol) in 200 ml of CH_2Cl_2 for 15 min. The resin was drained, washed with CH_2Cl_2 (5 ml × 3), DMF (5 ml × 3), and treated with a solution of peptide (1.2 equiv, 0.0015 mmol) and DIEA (10 equiv, 0.0125 mmol) in 400 ml DMF for 3 h. The peptide resin was drained and washed extensively with CH_2Cl_2 (5 ml × 3), DMF (5 ml × 3), CH_2Cl_2 (5 ml × 3) prior to screening.

Library synthesis. The library was constructed on TentaGel S NH_2 (RAPP Polymere, 0.25 mg ml⁻¹, 80 μm) using standard Fmoc chemistry. A linker ((β-alanine)-(6-aminocaproic)-Gly) and the biasing element (Asn-Asn-Tyr-Thr-Ser-Leu-Ile-His-Ser-Leu-Ile-Glu-Glu-Ser-Gln-Asn-Gln-Gln) were synthesized on 1.5 g (0.375 mmol) of resin. A modified recursive deconvolution strategy that allowed for the incorporation of 'skip codons' (no monomer addition) was used. The entire library was split into 50 portions by transferring 1 ml of a suspension of the resin in DMF (50 ml total volume of resin and solvent) to a reaction vessel (BioRad Bio-Spin® columns #732-6008). One vessel (skip codon) was kept aside, and monomers for position M2 were coupled to the 49 remaining portions. Each vessel was treated with a specific monomer (2 equiv, 0.015 mmol), HATU (2 equiv, 0.015 mmol) and DIEA (5 equiv, 0.0375 mmol) for 3 h in DMF (0.4 ml). The resin was washed DMF (5 ml × 3), CH_2Cl_2 (5 ml × 3), DMF (5 ml × 3), and then resubjected to monomer coupling under the same conditions but

Table 1 EC₅₀ for inhibition of gp41-mediated cell-cell fusion

	Peptide Sequence	EC₅₀
DP-178	[127]YTSLIHSLIEESQNQQEKNEQELLELDKWASLWNWF[162]	50 ± 22 nM
p38	[117]WMEWDREINNYTSLIHSLIEESQNQQEKNEQELLELDK[154]	2.7 ± 0.3 nM
C7Mn34Mn42p30	C7-Mn34-Mn42-NNYTSLIHSLIEESQNQQEKNEQELLELDK[154]	0.3 ± 0.1 μM
p30	[125]NNYTSLIHSLIEESQNQQEKNEQELLELDK[154]	6.6 ± 1.3 μM
p26	[117]WMEWDREINNYTSLIHSLIEESQNQQ[142]	2.8 ± 1.4 μM
C7Mn34Mn42p18	C7-Mn34-Mn42-NNYTSLIHSLIEESQNQQ[142]	>200 μM
p18	[125]NNYTSLIHSLIEESQNQQ[142]	>200 μM

for 12 h. The resin was finally washed with DMF (5 ml × 3), CH_2Cl_2 (5 ml × 3), DMF (5 ml × 3). 1.8 ml of DMF was added to each vessel, and 1.2 ml of the suspended resin was removed and pooled with other portions. The remaining one-third of the resin was left in the vessel, washed with DMF (5 ml × 3), CH_2Cl_2 (5 ml × 3), and stored in a vacuum desiccator. The pooled resin was subjected to 20% piperidine/DMF (7.5 ml) for 10 min, the solvent drained, and the resin retreated with 20% piperidine/DMF (7.5 ml) for another 5 min. The resin was extensively washed with several volumes of DMF, MeOH and CH_2Cl_2.

The pooled resin was split again into 50 portions, and 49 of the 50 vessels were treated as described above to react with the monomers corresponding to position M1. After coupling, 1.2 ml of DMF was added to each vessel and 0.6 ml of the suspended resin was removed and pooled. The remaining half was left in the vessel, washed with DMF (5 ml × 3), CH_2Cl_2 (5 ml × 3), and stored in a vacuum desiccator. The pooled resin was treated with 20% piperidine/DMF (7.5 ml) as described above.

The resin was split again into 50 equal portions. The resin in 24 of the 50 vessels was appropriately treated to react with the capping reagents corresponding to position C. Acid chlorides and chloroformates were coupled using the appropriate capping reagent (25 equiv, 0.0625 mmol) and DIEA (40 equiv, 0.1 mmol); sulfonyl chlorides were coupled using the capping reagent (10 equiv, 0.025 mmol) and triethylamine (20 equiv, 0.05 mmol); isocyanates were coupled using the capping reagent (25 equiv, 0.0625 mmol); anhydrides and carbamoyl chlorides were coupled using the capping reagent (30 equiv, 0.075 mmol) and DIEA (40 equiv, 0.1 mmol). All reactions were carried out in CH_2Cl_2 (0.4 ml). Acids were coupled using the capping reagent (5 equiv, 0.0125 mmol), HATU (4 equiv, 0.01 mmol), and DIEA (6 equiv, 0.015 mmol) in DMF (0.6 ml). Couplings were carried out for 18 h, and the resin was then washed with CH_2Cl_2 (5 ml × 3).

Side chain deprotection was carried out by treatment with 95% TFA, 2.5% H_2O, and 2.5% Et_3SiH for 3 h. After deprotection, the peptide resin was washed with CH_2Cl_2 (5 ml × 3), DMF (5 ml × 3), CH_2Cl_2 (5 ml × 3). The library was then dried under a stream of dry nitrogen and stored at -20 °C for further use.

Library screening and deconvolution. Position C of the library was deconvoluted by screening 25 discrete portions of the library (~6,000 beads, 2.3 copies). Each portion was first washed with DMF (5 ml × 3), i-PrOH (5 ml × 3), H_2O (5 ml × 3), PBST (5 ml × 3), and finally PBSTB. 0.2 ml of a premixed (10 min) solution of biotinylated gp41 inner core (2.7 μM) and streptavidin-alkaline phosphatase conjugate (SA-AP) (Pierce ImmunoPure streptavidin, alkaline phosphatase conjugate) (0.5 μM). After incubation for 2.5 h at 25 °C, beads were washed with 4 (10 s each) × 0.2 ml of PBSTB. Alkaline phosphatase substrate solution [5-bromo-4-chloro-3-indolyl-phosphate, p-toluidine (BCIP) and nitro-blue tetrazolium (NBT)] was added for 4 min, and the reaction was quenched with 6 M GdmHCl. Each portion of beads was analyzed under the microscope and scored for the darkest beads. Another set of 25 discrete portions of the library (~6,000 beads, 2.3 copies) was screened with SA-AP solution alone under conditions identical to those described above. Library portions with the highest number of darkest beads in the gp41/SA-AP screening and fewest dark beads in the SA-AP were selected for rescreening under more stringent conditions, using 0.9 μM biotinylated gp41 inner core and 0.16 μM SA-AP.

To deconvolute the M1 position, 50 portions of 0.000014 mmol of beads (1/18 of total saved from split prior to pooling the M1 position, ~1,600 beads) were subjected to coupling of the capping element selected in the deconvolution of position C. Each portion

was then acid deprotected and washed as described above. ~160 beads were washed and screened as described above for position C. To deconvolute the final position, M2, 50 portions of 0.00013 mmol of beads (1/20 of total saved from split prior to pooling the M2 position, ~1,400 beads) were subjected to coupling of the elements selected for positions M1 and C. Each portion was then acid deprotected and washed as described above, and 1/20 (~70 beads) beads were washed and screened as described above for position C.

Cell-cell fusion assay. A DNA clone of CD4 was obtained through the AIDS Research and Reference Reagent Program, Division of AIDS, NIAID, NIH, from R. Axel (Columbia University). T7 polymerase and encephalomyocarditis virus (EMCV) DNA were from ATCC (Rockville, MD). The luciferase gene pGL2 enhancer plasmid and luciferase assay system were from Promega (Madison, WI).

A luciferase reporter vector, pST7luc, was constructed by inserting a T7 promoter into pSP64 upstream of the cloning site. The internal ribosome entry site (IRES) from EMCV was then ligated in-frame to the 5' end of the gene for luciferase and downstream from the T7 promoter. The genes for CD4, T7 polymerase, and HIV-1 gp160$_{HXB}$ were subcloned into the mammalian expression vector, PMT3 (ref. 45).

The fusion assay was a modification of the reporter gene activation technique developed by Nussbaum *et al.*[46]. 293T cells were transfected by the calcium phosphate method in 10 cm dishes. Effector cells were cotransfected with equal amounts of gp160$_{HXB}$, and T7 polymerase, and target cells were cotransfected with pST7luc and CD4. As negative controls, either gp160$_{HXB}$ or CD4 were replaced in the transfection with the empty expression vector, PMT3. 40 h after addition of DNA precipitates, the cells were washed with serum free DMEM, then incubated 30–40 min with 9 ml/plate serum free DMEM at 37 °C. The cells were then gently dislodged from the plate by pipetting and pelleted in a clinical centrifuge. Each plate of cells was resuspended in 3–4 ml of DMEM with 10% FBS. 45 μl of target cells and 45 μl of effector cells were mixed in 96 well plates along with 10 μl of media (or PBS) with or without increasing concentrations of peptide. The peptides were dissolved in DMSO, then diluted 20-fold to their final stock concentration in PBS. Serial dilutions were made in media just prior to assay. The mixture of target cells, effector cells and inhibitor was agitated briefly, then incubated at 37 °C for 8 h. To assay luciferase activity, the medium was aspirated and the cells lysed in 60 μl of IX reporter lysis buffer (Promega). 40 μl of lysate was transferred to a black 96 well plate, and 100 μl of beetle luciferin and coenzyme A was added. Chemilluminescence was measured 2 min after addition of luciferase substrate in a 96 well plate reader attachment on a Spex fluorolog-3 fluorimeter using an emission wavelength of 552 nm and 7 mm slit widths. EC$_{50}$ values were estimated by fitting inhibition data to an equation for simple equilibrium binding: % luciferase activity = $100/(1+(C/EC_{50}))$.

articles

1. Dimitrov, D.S. How do viruses enter cells? The HIV coreceptors teach us a lesson of complexity. *Cell* **91**, 721–730 (1997).
2. Sattentau, Q.J. & Moore, J.P. Conformational changes induced in the human immunodeficiency virus envelope glycoprotein by soluble CD4 binding. *J. Exp. Med.* **174**, 407–415 (1991).
3. Sattentau, Q.J. & Moore, J.P. Conformational changes induced in the envelope glycoproteins of the human and simian immunodeficiency viruses by soluble receptor binding. *J. Virol.* **67**, 7383–7393 (1993).
4. Trkola, A. *et al.* CD4-dependent, antibody-sensitive interactions between HIV-1 and its co-receptor CCR-5. *Nature* **384**, 184–187 (1996).
5. Wu, L. *et al.* CD4-induced interaction of primary HIV-1 gp120 glycoproteins with the chemokine receptor CCR-5. *Nature* **384**, 179–183 (1996).
6. Littman, D.R. Chemokine receptors: Keys to AIDS pathogenesis? *Cell* **93**, 677–680 (1998).
7. Sullivan, N., *et al.* CD4-induced conformational changes in the human immunodeficiency virus type 1 gp120 glycoprotein: consequences for virus entry and neutralization. *J. Virol.* **72**, 4694–4703 (1998).
8. Chan, D.C., Fass, D., Berger, J.M. & Kim, P.S. Core structure of gp41 from the HIV envelope glycoprotein. *Cell* **89**, 263–273 (1997).
9. Weissenhorn, W., Dessen, A., Harrison, S.C., Skehel, J.J. & Wiley, D.C. Atomic structure of the ectodomain from HIV-1 gp41. *Nature* **387**, 426–430 (1997).
10. Tan, K., Liu, J.-H., Wang, J.-H., Shen, S. & Lu, M. Atomic structure of a thermostable subdomain of HIV-1 gp41. *Proc. Natl. Acad. Sci. USA* **94**, 12303–12308 (1997).
11. Bullough, P.A., Hughson, F.M., Skehel, J.J. & Wiley, D.C. Structure of influenza haemaglutinin at the pH of membrane fusion. *Nature* **371**, 37–43 (1994).
12. Joshi, S.B., Dutch, R.E. & Lamb, R.A. A core trimer of the paramyxovirus fusion protein: parallels to influenza virus hemagglutinin and HIV-1 gp41. *Virology* **248**, 20–34 (1998).
13. Dutch, R.E., Leser, G.P. & Lamb, R.A. Paramyxovirus fusion protein: characterization of the core trimer, a rod-shaped complex with helices in anti-parallel orientation. *Virology* **254**, 147–159 (1999).
14. Baker, K.A., Dutch, R.E., Lamb, R.A. & Jardetzky, T.S. Structural basis for paramyxovirus-mediated membrane fusion. *Mol. Cell* **3**, 309–319 (1999).
15. Weissenhorn, W., Carfí, A., Lee, K.-H., Skehel, J.J. & Wiley, D.C. Crystal structure of the Ebola virus membrane fusion, GP2, from the envelope glycoprotein ectodomain. *Mol. Cell* **2**, 605–616 (1998).
16. Malashkevich, V.N., *et al.* Core structure of the envelope glycoprotein GP2 from Ebola virus at 1.9A resolution. *Proc. Natl. Acad. Sci. USA* **96**, 2662–2667 (1999).
17. Fass, D., Harrison, S.C. & Kim, P.S. Retrovirus envelope domain at 1.7 angstrom resolution. *Nature Struct. Biol.* **3**, 465–469 (1996).
18. Center, R.J., *et al.* Crystallization of a trimeric human T cell leukemia virus type 1 gp21 ectodomain fragment as a chimera with maltose-binding protein. *Protein Sci.* **7**, 1612–1619 (1998).
19. Kobe, B., Center, R.J., Kemp, B.E. & Poumbourios, P. Crystal structure of human T cell leukemia virus type 1 gp21 ectodomain crystallized as a maltose-binding protein chimera reveals structural evolution of retroviral transmembrane proteins. *Proc. Natl. Acad. Sci. USA* **96**, 4319–4324 (1999).
20. Caffrey, M., *et al.* Three-dimensional solution structure of the 44kDa ectodomain of SIV gp41. *EMBO J.* **17**, 4572–4584 (1998).
21. Malashkevich, V.N., Chan, D.C., Chutkowski, C.T. & Kim, P.S. Crystal structure of the simian immunodeficiency virus (SIV) gp41 core: conserved helical interactions underlie the broad inhibitory activity of gp41 peptides. *Proc. Natl. Acad. Sci. USA* **95**, 9134–9139 (1998).
22. Skehel, J.J. & Wiley, D.C. Coiled coils in both intracellular vesicle and viral membrane fusion. *Cell* **95**, 871–874 (1998).
23. Hughson, F.M. Enveloped viruses: A common mode of membrane fusion? *Current Biology* **7**, 565–569 (1997).
24. Daniels, R.S. *et al.* Fusion mutants of influenza virus hemagglutinin glycoprotein. *Cell* **40**, 431–439 (1985).
25. Bodian, D.L. *et al.* Inhibition of the fusion-inducing conformational change of influenza hemagglutinin by benzoquinones and hydroquinones. *Biochemistry* **32**, 2967–2978 (1993).
26. Hoffman, L.R., Kuntz, I.D. & White, J.M. Structure-based identification of an inducer of low-pH conformational change in influenza virus hemagglutinin: irreversible inhibition of infectivity. *J. Virol.* **71**, 8808–8820 (1997).
27. Wild, C., Oas, T., McDanal, C., Bolognesi, D. & Matthews, T. A synthetic peptide inhibitor of human immunodeficiency virus replication: correlation between solution structure and viral inhibition. *Proc. Natl. Acad. Sci. USA* **89**, 10537–10541 (1992).
28. Wild, C.T., Shugars, D.C., Greenwell, T.K., McDanal, C.B. & Matthews, T.J. Peptides corresponding to a predictive α-helical domain of human immunodeficiency virus type 1 gp41 are potent inhibitors of virus infection. *Proc. Natl. Acad. Sci. USA* **91**, 9770–9774 (1994).
29. Gallaher, W.R., Ball, J.M., Garry, R.F., Griffin, M.C. & Montelaro, R.C. A general model for the transmembrane proteins of HIV and other retroviruses. *AIDS Res. Human Retroviruses* **5**, 431–440 (1989).
30. Kilby, J.M. *et al.* Potent suppression of HIV-1 replication in humans by T-20, a peptide inhibitor of gp41-mediated virus entry. *Nature Med.* **4**, 1302–1307 (1998).
31. Dubay, J.W., Roberts, S.J., Brody, B. & Hunter, E. Mutations in the leucine zipper of the human immunodeficiency virus type 1 transmembrane glycoprotein affect fusion and infectivity. *J. Virol.* **66**, 4748–4756 (1992).
32. Weng, Y. & Weiss, C.D. Mutational analysis of residues in the coiled-coil domain of human immunodeficiency virus type 1 transmembrane protein gp41. *J. Virol.* **72**, 9676–9682 (1998).
33. Chan, D.C., Chutkoski, C.T. & Kim, P.S. Evidence that a prominent cavity in the coiled coil of HIV type 1 gp41 is an attractive drug target. *Proc. Natl. Acad. Sci. USA* **95**, 15613–15617 (1998).
34. Combs, A.P., *et al.* Protein structure-based combinatorial chemistry: discovery of non-peptide binding elements to Src SH3 domain. *J. Am. Chem. Soc.* **118**, 287–288 (1996).
35. Feng, S., Kapoor, T.M., Shirai, F., Combs, A.P. & Schreiber, S.L. Molecular basis for the binding of SH3 ligands with non-peptide elements by combinatorial synthesis. *Chem. Biol.* **3**, 661–670 (1996).
36. Lam, K.S., Lebl, M. & Krchnák, V. The one bead-one-compound combinational library method. *Chem. Rev.* **97**, 411–448 (1997).
37. Erb. E., Janda, K.D. & Brenner, S. Recursive deconvolution of combinational chemical libraries. *Proc. Natl. Acad. Sci. USA* **91**, 11422–11426 (1997).
38. Lu, M., Blacklow, S.C. & Kim, P.S. A trimeric structural domain of the HIV-1 transmembrane glycoprotein. *Nature Struct. Biol.* **2**, 1075–1082 (1995).
39. Lawless, M.K. *et al.* HIV-1 membrane fusion mechanism: structural studies of the interactions between biologically-active peptides from gp41. *Biochemistry* **35**, 13697–13708 (1996).
40. Muñoz-Barroso, I., Durell, S., Sakaguchi, K., Appella, E. & Blumenthal, R. Dilation of the human immunodeficiency virus-1 envelope glycoprotein fusion pore revealed by the inhibitory action of a synthetic peptide from gp41. *J. Cell Biol.* **140**, 315–323 (1998).
41. Furuta, R.A., Wild, C.T., Weng, Y. & Weiss, C.D. Capture of an early fusion-active conformation of HIV-1 gp41. *Nature Struc. Biol.* **5**, 276–279 (1998).
42. Blacklow, S.C., Lu, M. & Kim, P.S. A trimeric subdomain of the simian immunodeficiency virus envelope glycoprotein. *Biochemistry* **34**, 14955–14962 (1995).
43. Weissenhorn, W., *et al.* Assembly of a rod-shaped chimera of a trimeric GCN4 zipper and the HIV-1 gp41 ectodomain expressed in *Escherichia coli. Proc. Natl. Acad. Sci. USA* **94**, 6065–6069 (1997).
44. Rimsky, L.T., Shugars, D.C. & Matthews, T.J. Determinants of human immunodeficiency virus type 1 resistance to gp41-derived inhibitory peptides. *J. Virol.* **72**, 986–993 (1998).
45. Franke, R.R., Sakmar, T.P., Oprian, D.D. & Khorana, H.G. A single amino acid substitution in rhodopsin (lysine 248-leucine) prevents activation of transducin. *J. Biol. Chem.* **263**, 2119–2122 (1988).
46. Nussbaum, O., Broder, C.C. & Berger, E.A. Fusogenic mechanisms of enveloped-virus glycoproteins analyzed by a novel recombinant vaccinia virus-based assay quantitating cell fusion-dependent reporter gene activation. *J. Virol.* **68**, 5411–5422 (1994).
47. Carson, M. & Bugg, C.E. Algorithm for ribbon models of proteins. *J. Mol. Graph.* **4**, 121–122 (1986).